BNL-222534-2021-JAAM

Exfoliating silica bilayers via intercalation at the silica/transition metal interface

M. Wang, D. Lu

To be published in "Nanotechnology"

December 2021

Center for Functional Nanomaterials

Brookhaven National Laboratory

U.S. Department of Energy

USDOE Office of Science (SC), Basic Energy Sciences (BES) (SC-22)

Notice: This manuscript has been authored by employees of Brookhaven Science Associates, LLC under Contract No.DE-SC0012704 with the U.S. Department of Energy. The publisher by accepting the manuscript for publication acknowledges that the United States Government retains a non-exclusive, paid-up, irrevocable, world-wide license to publish or reproduce the published form of this manuscript, or allow others to do so, for United States Government purposes.

DISCLAIMER

This report was prepared as an account of work sponsored by an agency of the United States Government. Neither the United States Government nor any agency thereof, nor any of their employees, nor any of their contractors, subcontractors, or their employees, makes any warranty, express or implied, or assumes any legal liability or responsibility for the accuracy, completeness, or any third party's use or the results of such use of any information, apparatus, product, or process disclosed, or represents that its use would not infringe privately owned rights. Reference herein to any specific commercial product, process, or service by trade name, trademark, manufacturer, or otherwise, does not necessarily constitute or imply its endorsement, recommendation, or favoring by the United States Government or any agency thereof or its contractors or subcontractors. The views and opinions of authors expressed herein do not necessarily state or reflect those of the United States Government or any agency thereof.

Exfoliating silica bilayers via intercalation at the silica/transition metal interface

Mengen Wang[1,2], J. Anibal Boscoboinik[1], and Deyu Lu[1*]

[1] Center for Functional Nanomaterials, Brookhaven National Laboratory, Upton, NY 11973, United States.
[2] Materials Science and Chemical Engineering Department, Stony Brook University, Stony Brook, NY 11790, United States.

E-mail: dlu@bnl.gov

Abstract

The growth of the silica (SiO_2) bilayer (BL) films on transition metal (TM) surfaces creates a new class of two-dimensional (2D) crystalline, self-contained materials that interact weakly with the TM substrate. The BL-silica/TM heterojunction has shown unique physical and chemical properties that can lead to new chemical reaction mechanisms under the sub-nm confinement and broad potential applications ranging from surface protection, nano transistors, molecular sieves to nuclear waste removal. Novel applications of BL-silica can be further explored as a constituent of van der Waals assembly of 2D materials. Key to these applications is an unmet technical challenge to exfoliate and transfer BL-silica films in a large area from one substrate to another without material damage. In this study, we propose a new exfoliation mechanism based on gas molecule intercalation from density functional theory studies of the BL-silica/TM heterojunction. We found that the intercalation of O atoms and CO molecules at the BL-silica/TM interface weakens the BL-silica – TM hybridization, which results in an exponential decrease of the exfoliation energy against the interface distance as the coverage of interfacial species increases. This new intercalation mechanism opens up the opportunity for non-damaging exfoliation and transfer of large area silica bilayers.

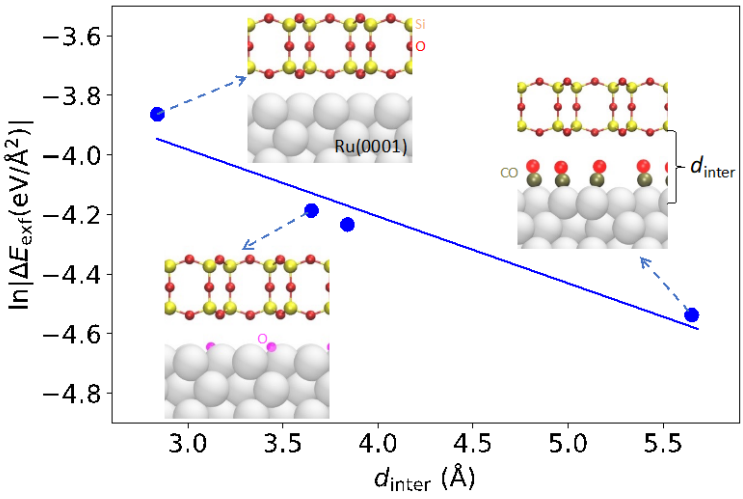

Graphic abstract

Keywords: zeolite, bilayer silica, exfoliation, density functional theory

 © xxxx IOP Publishing Ltd

1. Introduction

There have been intensive research efforts devoted to the synthesis of crystalline silica films on a variety of transition metal (TM) substrates, such as Mo, Cu, Ni, Pd, Pt, and Ru.[1-11] Monolayer films with the stoichiometry of $SiO_{2.5}$ can be grown on Mo and the system has strong Si-O-metal bonds.[1] To reduce the strong metal-silica interaction and maintain the SiO_2 stoichiometry, weakly interacting 2D bilayer (BL) silica films were synthesized on Pt[7] and Ru.[8] The BL-silica films consist of a 2D array hexagonal prism nanocages that has the [SiO_4] corner-sharing tetrahedra bonding motif.[5] The synthesis of the BL-silica film is achieved by evaporating Si onto the Ru(0001) surface at room temperature under 2×10^{-7} mbar of O_2[12, 13] followed by a crystallization step at 1200 K.[14]

The morphology of the silica film shows a strong dependence on the oxygen adsorption energy on the TM substrate.[1-11] Oxygen adatoms adsorb much stronger on Mo(112) than Pt(111)[15-18], with the calculated O adsorption energy of -1.3 eV on Pt(111)[17, 18] and -2.8 eV on Mo(112).[15, 16] As a result, only the monolayer silica film ($SiO_{2.5}$) with strong O-Mo bonds can be grown on Mo(112).[1] Similarly, the monolayer silica film can also be synthesized on Ni(111)[19] and Cu(111).[11] On the other hand, bilayer silica films can be synthesized on Ru(0001),[8, 20] Pd(111),[10] and Pt(111),[7] where the O-TM interaction is weaker. Interestingly, Ru(0001) has an intermediate oxophilicity, which allows the growth of both monolayer and bilayer.

The unique size of the nano-cage (~5.4 Å) of the BL-silica allows single-atom trapping of Ar, Kr, Xe, which is ideal for noble gas storage and separation applications.[13, 21] BL-silica interacts weakly with the metal substrates as the thickness of the interfacial space between them is over ~3 Å. This sub-nanosized space between BL-silica and TM support creates an ideal model system to study chemical reactions at confined spaces, such as CO oxidation and water formation reaction.[22-24] In addition, BL-silica/metal heterostructures have potential applications for surface protection[25], molecular sieves,[13, 26] and nano transistors (due to silica's wide band gap of ~6.5 eV[27]). The materials space of the 2D silica family can be future expanded into, e.g., vertically stacked van der Waals (vdW) heterostructures to achieve new material properties with 2D silica as one constituent. Essential to the practical utility of these new materials platforms is a non-damaging method to exfoliate large areas of the 2D silica film from its substrate that allows it to be transferred onto a new substrate.

Mechanical exfoliation has been widely used to obtain high-quality structures of single layer MoS_2,[28] $MoSe_2$,[29] and graphene[30] from bulk crystals. A poly methyl methacrylate (PMMA) assisted transfer of the amorphous BL-silica from Ru(0001) to Pt(111) has been reported at the millimeter scale, which takes advantage of its weak interaction with the TM substrate.[31] The exfoliation energy of the BL-silica film on the Ru(0001) substrate was overcome by the adhesion between the PMMA film and the BL-silica film. Nevertheless, exfoliation of the crystalline BL-silica films, instead of the amorphous BL-silica, which is crucial to practical applications, has not been demonstrated. It has been proposed to explore various substrate and polymer combinations in order to reduce the exfoliation energy between substrate and BL-silica and/or increase the adhesion strength between the polymer and BL-silica.[31] However, this material space is quite restricted due to the limited choice of TM substrates suitable for the synthesis.

Due to the nano-porous structures of the BL-silica and the weak interaction between BL-silica and TM substrates (e.g., Ru, Pd and Pt), small entities such as Cu,[32] Au, Pd[33] atoms, and O_2[12, 34] and CO[26, 35] molecules can penetrate through the nano-cages and reach the BL-silica/TM interface. O_2 molecules on Ru(0001) surfaces can then dissociate into atomic O, with preferential adsorption on the *hcp*-hollow sites for coverages between 0.25 monolayer (ML) and 1 ML.[36-38] The same process on Pd(111) and Pt(111) leads to preferential adsorption on the *fcc*-hollow sites.[39-42] The surface oxygen coverage on Pd(111) varies from 0.25 ML to 1 ML.[43-45] CO adsorption at the BL-silica/Ru(0001) interface was studied by infrared reflection absorption spectroscopy (IRRAS), and the peak at 2051 cm^{-1} observed from the exposure to 2×10^{-6} mbar CO at 300 K was assigned to the CO coverage of 0.5 ML.[26, 35] The presence of the interfacial O atoms increases separation between the BL-silica and the TM support, decreasing their interaction, as previously shown for Ru(0001).[12, 46] This, in turn, can lower the exfoliation energies of BL-silica.

In this work, we propose a gas molecule intercalation method to reduce the exfoliation energy of the BL-silica on TM substrates. We explored the exfoliation mechanism of intercalation of interfacial O atoms and CO molecules at various coverages at the BL-silica/Ru(0001) interface. We found that the exfoliation energy decays exponentially at the increasing interface distance between BL-silica and Ru(0001), as the coverage of interfacial O or CO increases. We also found that the charge rearrangement at the BL-silica/Ru(0001) interface is strongly influenced by the interface distance. This effect can be characterized by the p_z band shift of the BL-silica, which serves as a descriptor for the exfoliation energy. The key conclusions of the intercalation mechanism can be extended to Pd(111) and Pt(111) substrates. Our study suggests that gas phase (atom or molecule) intercalation at the BL-silica/TM interface is a promising method to achieve non-damaging BL-silica exfoliation.

2. Computational Methods

 © xxxx IOP Publishing Ltd

Density Functional Theory (DFT) calculations were performed using projector augmented-wave (PAW) method implemented in the Vienna *Ab initio* simulation package (VASP).[47, 48] The vdW-DF-cx functional[49, 50] was used to treat the non-local vdW interactions at the BL-silica/TM heterojunction. The Brillouin zone was sampled with an 8×4×1 k-point grid and a kinetic energy cutoff of 800 eV was used. The TM substrates were modeled with five layers. The lattice parameters are a = 5.39 Å, b = 9.34 Å and c = 27 Å for Ru, a = 5.50 Å, b = 9.52 Å and c = 27 Å for Pd and a = 5.56 Å, b = 9.62 Å and c = 27 Å for Pt. The vacuum thickness is set to ~10 Å. During the structure optimization, the top two layers of the substrate and the BL-silica film were fixed, with the rest of the system relaxed until the interatomic forces were smaller than 0.01 eV/Å. The dipole correction method[51] was applied to remove the spurious electrostatic interactions with image cells in the surface normal direction.

3. Results and Discussions

Here we quantify the impact of the O and CO intercalation on the exfoliation energy of the BL-silica on Ru, Pd and Pt substrates. We further analyse the charge rearrangement at the BL-silica/TM interface to provide the electronic structure details. We mainly present the results from BL-silica/Ru(0001). The equivalent cases but on Pd(111) and Pt(111) are included in the Supplementary Information.

3.1 Exfoliation energy of the BL-silica from TM substrates

The interface distance of the BL-silica/Ru(0001) heterojunction can be modified by varying the adsorbed O (θ_{Oads}) and CO coverage (θ_{CO}) on the Ru(0001) surface. Here, we define n_O (n_{CO}) as the number of O_{ads} atoms (CO molecules) per unit cell used in the calculation.

In order to compute the exfoliation energies at various θ_{Oads}, three systems (BL-silica/n_OO/Ru) were built, where n_O = 0 [Figure 1(a)] corresponds to clean Ru(0001) surface (θ_{Oads} = 0 ML), n_O = 2 [Figure 1(b)] corresponds to $p(2 \times 2)$-O/Ru(0001)[36] (θ_{Oads} = 0.25 ML), and n_O = 4 [Figure 1(c)] corresponds to $p(2 \times 1)$-O/Ru(0001) (θ_{Oads} = 0.5 ML).[37] Our previous studies have shown that the interface distance (d_{inter}), defined as the distance between the top layer of the substrate and the bottom layer O of the BL-silica (O_{bot}), increases from 2.84 Å to 3.84 Å as θ_{Oads} increases from 0 to 0.5 ML.[12] The increase in d_{inter} results in a decrease in the interface charge transfer and a weaker O-Ru hybridization.[12] Our work also showed that experimentally θ_{Oads} can be achieved up to 0.75 ML, and can be tuned by varying the O_2 pressure.[12] In this work, we calculated exfoliation energies as $\Delta E_{exf} = E_{MS\text{-}silica} - (E_{MS} + E_{silica})$, where the energies of the subsystems are obtained after structure optimization and E_{MS} corresponds to the total energy of the metal substrate (M) plus the surface species (S: O or CO). ΔE_{exf} changes from -0.021 eV/Å^2 (θ_{Oads} = 0 ML) to -0.015 eV/Å^2 (θ_{Oads} = 0.25 and 0.5 ML). ΔE_{exf} of the BL-silica bilayer is comparable to the range of $\Delta E_{exf} \sim -0.018$ eV/Å^2 of graphene adsorbed on the fcc metal (111) surface of Ni, Cu, Pd, Pt, Ag, and Au[52] calculated using the vdW-DF2 functional.[53] We have estimated the phonon contribution, including the vibrational energy and the entropy due to the vibrational degrees of freedom, to the Helmholtz free energy under the harmonic approximation for the surface with no O (silica/0O/Ru) and with 0.5 monolayer O (silica/4O/Ru) adsorbed at the silica/Ru interface. We found that the temperature effects are unimportant to the exfoliation, although the overall trend is to slightly reduce the exfoliation energy. For example, at T = 298 K, the phonon contribution causes a decrease of $|\Delta E_{exf}|$ by 0.0008 eV/Å^2 for silica/0O/Ru and 0.0021 eV/Å^2 for silica/4O/Ru, as compared to $|\Delta E_{exf}|$ of 0.0210 eV/Å^2 and 0.0145 eV/Å^2 without considering the phonon contribution. We also note that the phonon contribution is nearly the same for both systems, which will not affect our proposed mechanism of using O and CO intercalation to assist the exfoliation process.

Since CO molecules can penetrate through the nano-cages of the BL-silica and subsequently adsorb at the BL-silica/Ru(0001) interface, it is likely that CO molecules can also reduce the BL-silica – Ru(0001) interaction and lower the exfoliation energy. We investigated various CO coverages (BL-silica/n_{CO}CO/Ru), where n_{CO} is 3 [θ_{CO}= $\frac{3}{8}$ ML, Figure 1(d)], 4 [θ_{CO}= $\frac{1}{2}$ ML, Figure 1(e)], 5 [θ_{CO}= $\frac{5}{8}$ ML, Figure 1(f)], and 8 [θ_{CO}=1 ML, Figure 1(g)]. In our atomic models, there are eight surface Ru atoms in the cell. For example, at θ_{CO} = $\frac{3}{8}$ ML, $\frac{2}{3}$ of the adsorbed CO molecules are adsorbed under the pores of BL-silica, while the rest $\frac{1}{3}$ block the interaction between O_{bot} and Ru(0001), which drastically increases d_{inter} to 5.65 Å as compared to 2.84 Å without CO intercalation. As a result, ΔE_{exf} reduces from -0.021 eV/Å^2 (θ_{CO}= 0 ML) to -0.011 eV/Å^2 (θ_{CO}= $\frac{3}{8}$ ML) due to the weaker BL-silica-Ru interactions. As shown in Figure 2(a), $|\Delta E_{exf}|$ decays exponentially as a function of d_{inter} in ther range of 2.84 Å (θ_{CO}= 0 ML) and 5.65 Å (θ_{CO}= $\frac{3}{8}$ ML). The trend can be fitted to $|\Delta E_{exf}| = 0.037\, e^{-0.22 d_{inter}}$ (eV/Å^2). When θ_{CO} is lower than $\frac{3}{8}$ ML, CO molecules cannot lift up the BL-silica film [see Figure S1 (a) and (c) as compared to Figure S1 (b) and (d)], and do not reduce $|\Delta E_{exf}|$. We therefore do not consider configurations at $\theta_{CO} < \frac{3}{8}$ ML in the following discussions.

We found that $|\Delta E_{exf}|$ saturates at high CO coverages, when d_{inter} reaches 5.97 Å [θ_{CO}= $\frac{1}{2}$ ML in Figure 1(e)] and

 © xxxx IOP Publishing Ltd

6.07 Å [$\theta_{CO}=\frac{5}{8}$ ML in Figure 1(f)], and slightly increases at d_{inter}=6.21 Å [θ_{CO}= 1 ML in Figure 1(g)], as indicated by purple triangles in Figure 2(a). The reason is that at large θ_{CO}, while the interaction energy between the BL-silica and Ru ($\Delta E_{silica/Ru}$) decreases, the interaction energy between CO and the BL-silica ($\Delta E_{silica/CO}$) increases more rapidly. To quantify this effect, we calculated $\Delta E_{silica/CO} = E_{silica/CO} - (E_{CO} + E_{silica})$. The corresponding structures of BL-silica/CO systems were taken from the relaxed BL-silica/ n_O O(n_{CO} CO)/Ru systems. We also calculated $\Delta E_{silica/Ru} = E_{silica/Ru} - (E_{Ru} + E_{silica})$. At d_{inter} = 2.84, 3.65, 3.84, 5.65, 5.97, 6.07 and 6.21 Å, the structures were taken from the BL-silica/n_OO(n_{CO}CO)/Ru systems. We included three more systems with d_{inter} = 3.24, 4.45 and 5.05 Å to provide more data points. As there is no O or CO adsorbed structures on the metal that can yield these interface distances, the structures are built by taking the structure of BL-silica/0O/Ru and manually increasing d_{inter}.

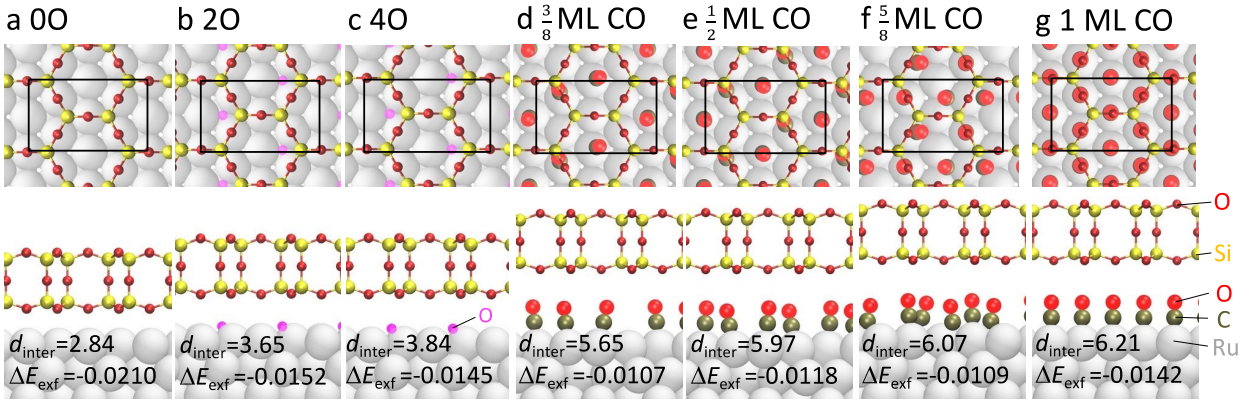

Figure 1. Top (top) and side (bottom) view of the relaxed structures of BL-silica/n_OO(n_{CO}CO)/Ru(0001) with (a) n_O = 0, (b) n_O = 2, (c) n_O = 4, (d) n_{CO} = 3, (e) n_{CO} = 4, (f) n_{CO} = 5, and (g) n_{CO} = 8. Color code: Ru (white), Si (yellow), O from silica bilayer and CO (red), O_{sur} (pink) and C (tan). d_{inter} (Å) represents the interface distance and ΔE_{exf} (eV/Å^2) is the exfoliation energy.

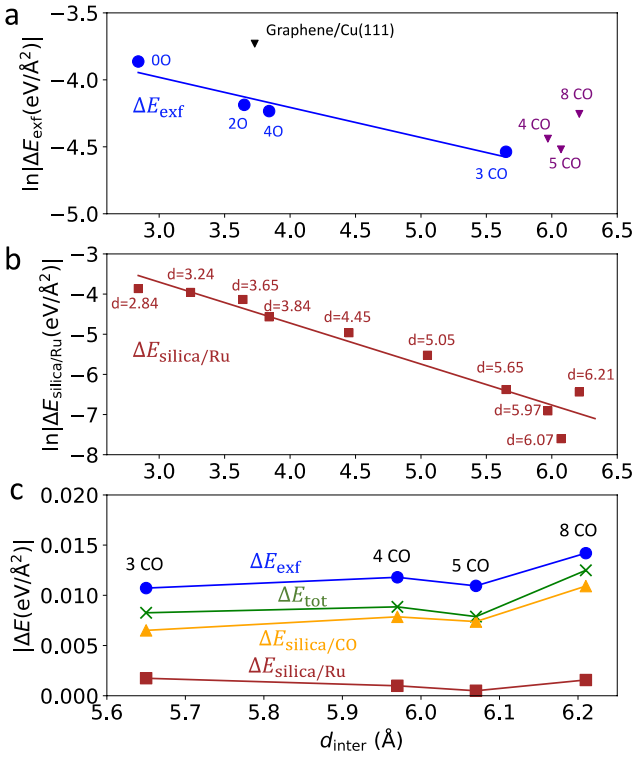

Figure 2 **(a)** The absolute value of the exfoliation energies ($|\Delta E_{exf}|$) (blue dots and purple down triangles) versus the interface distances (d_{inter}) between the bilayer silica and Ru. As a reference, the exfoliation energy of graphene on Cu(111) is indicated by the black down triangle. **(b)** The interaction energies ($|\Delta E_{silica/Ru}|$ in brown squares) between Ru and BL-silica versus d_{inter}. $|\Delta E_{exf}|$ and $|\Delta E_{silica/Ru}|$ as a function of d_{inter}. **(c)** The absolute value of the exfoliation energies ($|\Delta E_{exf}|$ in blue dots), interaction energies between Ru and BL-silica ($|\Delta E_{silica/Ru}|$ in brown squares), interaction energies between CO and BL-silica ($|\Delta E_{silica/CO}|$ in orange triangles) and the sum of $|\Delta E_{silica/Ru}|$ and $|\Delta E_{silica/CO}|$ (green x) versus d_{inter} for BL-silica/n_{CO}CO/Ru. All the energies are in eV/Å^2.

As shown in Figure 2(b), $|\Delta E_{silica/Ru}|$ decays exponentially as $0.527e^{-1.02\,d_{inter}}$ (eV/Å^2). The tail of this curve, corresponding to the range of $\theta_{CO} \geq \frac{3}{8}$ ML, is shown in the brown curve in Figure 2(c). Clearly, further increase in d_{inter} at high CO coverages will not further decrease $|\Delta E_{exf}|$. On the other hand, $|\Delta E_{silica/CO}|$ [orange curve in Figure 2(c)] becomes larger as θ_{CO} increases, which overweighs the opposite contribution from $|\Delta E_{silica/Ru}|$. As shown in Figure 2(c), the sum of $|\Delta E_{silica/CO}|$ and $|\Delta E_{silica/Ru}|$ (green) follows the trend in $|\Delta E_{exf}|$ (blue), where $\Delta E_{silica/CO}$ dominates in ΔE_{exf} at $\theta_{CO} \geq \frac{3}{8}$ ML and causes $|\Delta E_{exf}|$ to saturate and even slightly increase. At $\theta_{CO} = \frac{5}{8}$ ML, the calculated CO bond length is 1.18 Å, which is consistent with the previous DFT study (1.16 Å at $\theta_{CO} = \frac{5}{8}$ ML).[35] $\theta_{CO} = \frac{1}{2}$ ML can be achieved experimentally: the 2051 cm^{-1} peak from the Infrared

 © xxxx IOP Publishing Ltd

absorption spectra is assigned to the CO coverage of $\frac{1}{2}$ ML.[26, 35] ΔE_{exf} (~-0.01 eV/Å^2) is reduced by 50% when compared to the same system without adsorbates (~-0.02 eV/Å^2).

Similar studies were performed for BL-silica/Pd(111) and BL-silica/Pt(111) interfaces as shown in Figures. S2 and S3 in the Supplementary Information. In summary of all the results, ΔE_{exf} follows a universal exponential trend as a function of d_{inter}, $|\Delta E_{exf}| = 0.04\, e^{-0.28 d_{inter}}$ (eV/Å^2), regardless of the TM substrates (Pd, Pt, and Ru) as shown in Figure 3. Without adsorbates, $|\Delta E_{exf}|$ is the lowest on Pt(111) (0.019 eV/Å^2) followed by Ru(0001) (0.021 eV/Å^2) and Pd (111) (0.021 eV/Å^2). In the presence of interfacial CO with $\theta_{CO} = \frac{3}{8}$ ML, the lowest $|\Delta E_{exf}|$ is found at the BL-silica/3CO/Pt(111) interface (0.008 eV/Å^2), which indicates that it is easiest to exfoliate the BL-silica from the Pt(111) substrate.

The presence of defects could potentially result in slightly different exfoliation energies. Defects in the bilayer silica film are mainly non-six-member rings, for example, five, seven or eight-membered rings.[54] The non-six-member rings may have fewer or weaker O_{bot}-Ru bonds at the interface, which potentially reduce the exfoliation energy. There are a number of other factors that could also affect the exfoliation energy, including density of steps edges and how they interact with the silicate, the presence of step bunches, and the size and termination of domains, which set the basis for further studies under less ideal conditions.

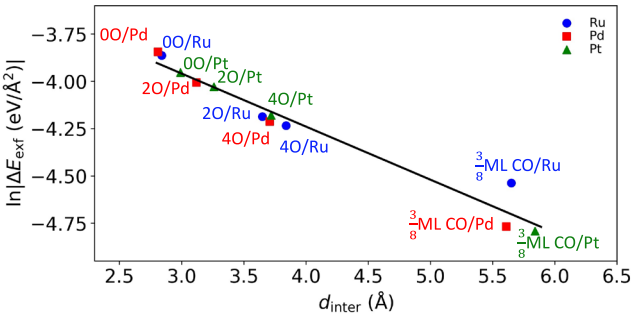

Figure 3 Dependence of exfoliation energies ($|\Delta E_{exf}|$ in eV/Å^2) on the interface distances (d_{inter}). Data include different transition metal substrates (Ru, Pd, and Pt) and interfacial species (O and CO), i.e., BL-silica/n_OO(n_{CO}CO)/Ru, BL-silica/n_OO(n_{CO}CO)/Pd and BL-silica/n_OO(n_{CO}CO)/Pt at $n_O = 0$, $n_O = 2$, $n_O = 4$, and $n_{CO} = 3$.

3.2 Charge rearrangement at the BL-silica/TM interface

To shed light on the electronic properties at the different BL-silica/TM interfaces, we studied the interfacial charge rearrangement. The BL-silica interacts with the substrate mainly via vdW forces due to the large interface distance of ~3 Å. In addition, our previous studies show that there is a charge rearrangement at the BL-silica/Ru(0001) interface, and the amount of interface charge transfer is 0.21 e$^-$/unit cell at the BL-silica/Ru(0001) interface.[12, 46] This interfacial charge transfer could be blocked by O_{ads}.[12, 46]

There are two types of Ru atoms present: Ru atoms under O_{bot} (Ru_O) and under the pores (Ru_{pore}), and they behave differently in the O-Ru hybridization as shown in Figure 4(a). There is an electron depletion in p_z orbitals of O_{bot} and d_{z^2} and s orbitals of Ru_O (regions in blue), and an electron accumulation in d_{xz} and d_{yz} orbitals of Ru_O and d_{z^2} and s orbitals of Ru_{pore} (regions in red). The origin of the charge rearrangement can be rationalized by the projected density of states (PDOS) as shown in Figure 4(b-e). Based on our previous studies of the BL-silica/Ru interface,[46] the charge redistribution can be attributed to two effects. Firstly, the p_z lone pair of O_{bot} [Figure 4(b)] hybridizes with Ru_O d_{z^2} and s states [Figure 4(c)], forming a bonding orbital (σ) dominated by the O_{bot} p_z character.[46] Secondly, the p_z lone pair of O_{bot} pushes the Ru_O d_{z^2} and s orbital to antibonding orbital (σ*) with a higher energy.[46] Consequently, electrons in the Ru_O d_{z^2} and s orbitals are partially transferred into the orbitals with lower energies in Ru_O d_{xz} and d_{yz} as well as Ru_{pore} d_{z^2}, as evidenced by the decrease in the occupied state as shown in Figure 4(c) and the increase in the occupied orbital as shown in Figure 4(d) and (e).

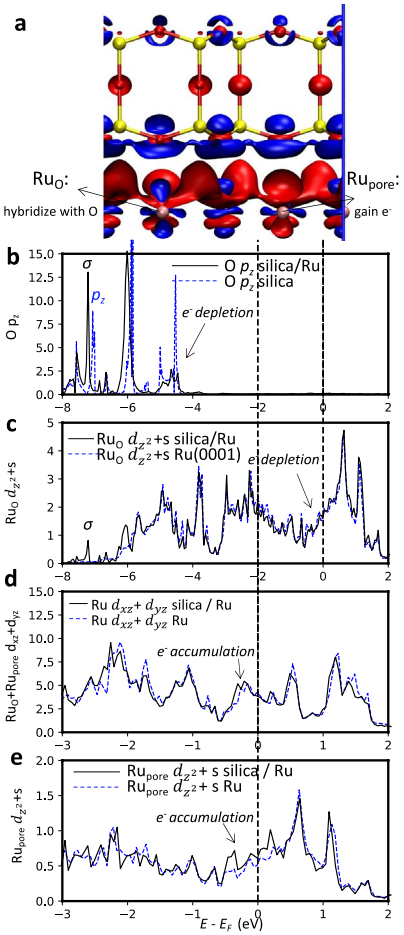

 © xxxx IOP Publishing Ltd

Figure 4 (a) Isosurface plot of the charge density difference upon adsorption of BL-silica on Ru(0001). The isodensity value is 0.005 e/Å^3. Red: electron accumulation regions; blue: electron depletion regions. Projected density of states of (b) O_{bot} p_z, (c) Ru_O $d_{z^2}+s$, (d) Ru $d_{xz}+d_{yz}$, and (e) Ru_{pore} $d_{z^2}+s$ orbitals before (dotted blue curve) and after (solid black curve) the BL-silica adsorption. The VBM of the freestanding silica bilayer is shifted to the VBM of the adsorbed BL-silica film.

An electronic signature of the hybridization between O_{bot} p_z and Ru_O d_{z^2} and s orbitals is the electron depletion at the O_{bot} p_z valence band maximum (VBM_{p_z}) at the BL-silica/Ru(0001) interface as shown in Figure 4(b). In the presence of the interfacial O atoms and CO molecules, the hybridization between O_{bot} and Ru_O is reduced and the electron depletion at VBM_{p_z} gradually disappears, as shown by the arrows in Figure 5, where the PDOS of the O_{bot} p_z band recovers. It is also important to note that VBM_{p_z} moves closer to the Fermi level in the presence of the surface species due to the decrease of the total interfacial dipole moment (p_{tot}) of BL-silica/n_OO(n_{CO}CO)/Ru(0001).[12] We obtained similar results at BL-silica/Pd(111) and BL-silica/Pt(111) interfaces as shown in Figure S4 of the Supplementary Information.

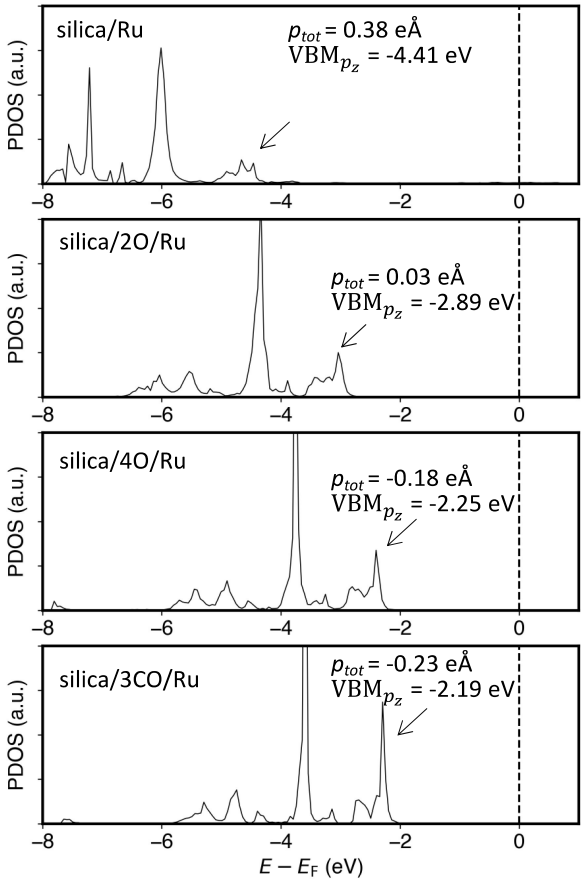

Figure 5 Projected density of states of p_z orbitals of the bottom layer O atoms. p_{tot} represent the total dipole moment of the system. VBM_{p_z} is the valence band maximum of the O_{bot} p_z orbital. The energies are relative to the Fermi level of BL-silica/n_OO(n_{CO}CO)/Ru(0001).

3.3 BL-silica O_{bot} p_z valence band center as a descriptor for the exfoliation energy

As a result of the hybridization between O_{bot} p_z and TM_O (the transition metal atom underneath O_{bot}) d_{z^2} and s orbitals, electron depletion happens at the valence band maximum (VBM) of the O_{bot} p_z band, which causes it shifted to lower energies, as compared to the freestanding BL-silica film. Due to the weaker hybridization and smaller charge transfer at the BL-silica/Pt(111) interface, the shift of the p_z band relative to the Fermi level as well as $|\Delta E_{exf}|$ are the smallest at BL-silica/Pt(111) than BL-silica/Pd(111) and BL-silica/Ru(0001). It is then expected that, after the intercalation of O atoms and CO molecules, the hybridization between O_{bot} and TM_O is partially blocked and the O_{bot} p_z band center will move back to higher energies. Consequently, one can correlate the O_{bot} p_z band center (ϵ_{p_z}) with ΔE_{exf}. Note that VBM of the BL-silica film moves closer to the Fermi level due to the decrease of the total dipole moment of at the BL-silica/ n_O O(n_{CO} CO)/TM interface.[12] This shift of VBM_{p_z}, however, does not contribute to the bonding between the BL-silica film and the substrate or ΔE_{exf}. Therefore, the O_{bot} p_z band center shift ($\Delta\epsilon_{p_z}$) is defined relative to VBM_{p_z} as $\Delta\epsilon_{p_z} = \frac{\int_{-\infty}^{VBM_{p_z}} DOS(E)*E}{\int_{-\infty}^{VBM_{p_z}} DOS(E)} - VBM_{p_z}$, to eliminate the effect from the interface dipole or VBM_{p_z} shift.

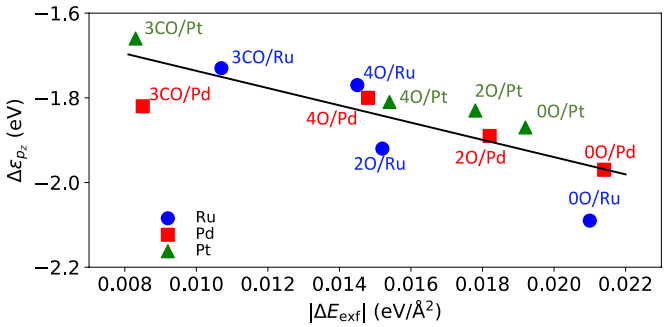

Figure 6 The O_{bot} p_z band center shift ($\Delta\epsilon_{p_z}$ in eV) versus the exfoliation energy ($|\Delta E_{exf}|$) for Ru, Pd and Pt at n_O = 0, n_O = 2, n_O = 4, and n_{CO} = 3.

The PDOS for the O_{bot} p_z orbitals are plotted for n_O = 0 (θ_{Oads} = 0 ML), n_O = 2 (θ_{Oads} = 0.25 ML), n_O = 4 (θ_{Oads} = 0.5 ML), and n_{CO} = 3 (θ_{CO}= $\frac{3}{8}$ ML) at the BL-silica/n_OO(n_{CO}CO)/TM in Figure 5 and Figure S4. Because the O_{bot} p_z and Ru d_{z^2}+s hybridization is the strongest at the BL-silica/Ru(0001), $\Delta\epsilon_p$=-2.09 eV is largest in magnitude as compared to -1.97 eV at BL-silica/Pd(111) and -1.87 eV at BL-silica/Pt(111). As θ_{Oads} and θ_{CO} increase from θ_{Oads}=0

 © xxxx IOP Publishing Ltd

ML to θ_{Oads} = 0.5 ML and θ_{CO}= $\frac{3}{8}$ ML, the σ peak becomes weaker and the electron depletion at the VBM becomes smaller. Therefore, $\Delta\epsilon_p$ increases as θ_{Oads} and θ_{CO} increase from θ_{Oads}=0 ML to θ_{CO}= $\frac{3}{8}$ ML, by 0.15 eV at the BL-silica/Pd(111) interface and by 0.21 eV at the BL-silica/Pt(111) interface, which is smaller than the increase of 0.36 eV at the BL-silica/Ru(0001) interface. Since ΔE_{exf} is larger under a stronger interfacial hybridization, $\Delta\epsilon_p$ anti-correlates with $|\Delta E_{exf}|$, which can be fitted to a straight line as shown in Figure 6. The deviation from the fitted line mainly comes from slightly different slopes from different metal substrates. Additionally, the hybridization almost vanishes at θ_{Oads} = 0.5 ML and vdW interactions become more significant in ΔE_{exf} at larger d_{inter}, which also introduce variations to the slope.

4. Conclusions

Our study provides insights into the exfoliation of the BL-silica based on the first principles analysis of the interaction between the BL-silica and the transition metal substrates. Intercalation of O atoms and CO molecules at the BL-silica/TM interface can modify the magnitude of the exfoliation energy, which decreases exponentially as the interfacial spacing increases in the presence of adsorbed species on the transition metal. A 50% reduction in exfoliation energy can be achieved when $\frac{3}{8}$ ML of CO are adsorbed at the BL-silica/TM interface, when compared the clean transition metal surfaces. This exfoliation energy (-0.011 eV/Å^2) is smaller in magnitude than that of graphene on Cu(111) (-0.018 eV/Å^2), indicating a good chance of success when attempted experimentally. Among the three TM substrates studied, Pt(111) yields the lowest exfoliation energy as compared to Pd(111) and Ru(0001). The degree of the BL-silica-TM hybridization and interfacial charge transfer decreases as the exfoliation energy decreases. The overall trend can be explained by an electronic descriptor defined as the p_z band center position of the bottom oxygen layer in the BL-silica. Our work provides important guidelines to achieving large-area, non-damaging, exfoliation of BL-silica from metals by pre-treating the sample with gas molecule intercalation prior to the exfoliation attempt. Upon experimental validation, this exfoliation method can lead to a wide range of applications.

Acknowledgment

This research used resources of the Center for Functional Nanomaterials, which is a U.S. DOE Office of Science Facility, and the Scientific Data and Computing Center, a component of the Computational Science Initiative, at Brookhaven National Laboratory under Contract No. DE-SC0012704. This research also used resources of the National Energy Research Scientific Computing Center (NERSC), a DOE Office of Science User Facility supported by the Office of Science of the U.S. Department of Energy under Contract No. DE-AC02-05CH11231.

References

1. Weissenrieder, J.; Kaya, S.; Lu, J. L.; Gao, H. J.; Shaikhutdinov, S.; Freund, H. J.; Sierka, M.; Todorova, T. K.; Sauer, J., Atomic Structure of a Thin Silica Film on a Mo(112) Substrate: A Two-Dimensional Network of SiO_4 Tetrahedra. *Physical Review Letters* **2005,** *95* (7), 076103.
2. Stacchiola, D.; Kaya, S.; Weissenrieder, J.; Kuhlenbeck, H.; Shaikhutdinov, S.; Freund, H.-J.; Sierka, M.; Todorova, T. K.; Sauer, J., Synthesis and Structure of Ultrathin Aluminosilicate Films. *Angewandte Chemie International Edition* **2006,** *45* (45), 7636-7639.
3. Kundu, M.; Murata, Y., Growth of single-crystal SiO_2 film on Ni(111) surface. *Applied Physics Letters* **2002,** *80* (11), 1921-1923.
4. Zhang, Z.; Jiang, Z.; Yao, Y.; Tan, D.; Fu, Q.; Bao, X., Preparation and characterization of atomically flat and ordered silica films on a Pd(100) surface. *Thin Solid Films* **2008,** *516* (12), 3741-3746.
5. Yang, B.; Kaden, W. E.; Yu, X.; Boscoboinik, J. A.; Martynova, Y.; Lichtenstein, L.; Heyde, M.; Sterrer, M.; Wlodarczyk, R.; Sierka, M.; Sauer, J.; Shaikhutdinov, S.; Freund, H.-J., Thin silica films on Ru(0001): monolayer, bilayer and three-dimensional networks of [SiO4] tetrahedra. *Physical Chemistry Chemical Physics* **2012,** *14* (32), 11344-11351.
6. Boscoboinik, J. A.; Yu, X.; Yang, B.; Fischer, F. D.; Włodarczyk, R.; Sierka, M.; Shaikhutdinov, S.; Sauer, J.; Freund, H.-J., Modeling Zeolites with Metal-Supported Two-Dimensional Aluminosilicate Films. *Angewandte Chemie International Edition* **2012,** *51* (24), 6005-6008.
7. Yu, X.; Yang, B.; Anibal Boscoboinik, J.; Shaikhutdinov, S.; Freund, H.-J., Support effects on the atomic structure of ultrathin silica films on metals. *Applied Physics Letters* **2012,** *100* (15), 151608.
8. Löffler, D.; Uhlrich, J. J.; Baron, M.; Yang, B.; Yu, X.; Lichtenstein, L.; Heinke, L.; Büchner, C.; Heyde, M.; Shaikhutdinov, S., Growth and structure of crystalline silica sheet on Ru (0001). *Physical Review Letters* **2010,** *105* (14), 146104.
9. Altman, E. I.; Götzen, J.; Samudrala, N.; Schwarz, U. D., Growth and characterization of crystalline silica films on Pd (100). *The Journal of Physical Chemistry C* **2013,** *117* (49), 26144-26155.

 © xxxx IOP Publishing Ltd

10. Jhang, J.-H.; Zhou, C.; Dagdeviren, O. E.; Hutchings, G. S.; Schwarz, U. D.; Altman, E. I., Growth of two dimensional silica and aluminosilicate bilayers on Pd (111): from incommensurate to commensurate crystalline. *Physical Chemistry Chemical Physics* **2017,** *19* (21), 14001-14011.
11. Navarro, J. J.; Tosoni, S.; Bruce, J. P.; Chaves, L.; Heyde, M.; Pacchioni, G.; Roldan Cuenya, B., Structure of a Silica Thin Film on Oxidized Cu (111): Conservation of the Honeycomb Lattice and Role of the Interlayer. *The Journal of Physical Chemistry C* **2020,** *124* (38), 20942-20949.
12. Wang, M.; Zhong, J.-Q.; Kestell, J.; Waluyo, I.; Stacchiola, D. J.; Boscoboinik, J. A.; Lu, D., Energy level shifts at the Silica/Ru (0001) heterojunction driven by surface and interface dipoles. *Topics in Catalysis* **2017,** *60* (6-7), 481-491.
13. Zhong, J.-Q.; Wang, M.; Akter, N.; Kestell, J. D.; Boscoboinik, A. M.; Kim, T.; Stacchiola, D. J.; Lu, D.; Boscoboinik, J. A., Immobilization of single argon atoms in nano-cages of two-dimensional zeolite model systems. *Nature Communications* **2017,** *8*, 16118.
14. Boscoboinik, J. A.; Yu, X.; Yang, B.; Fischer, F. D.; Włodarczyk, R.; Sierka, M.; Shaikhutdinov, S.; Sauer, J.; Freund, H.-J., Modeling Zeolites with Metal-Supported Two-Dimensional Aluminosilicate Films. *Angew. Chem. Int. Ed.* **2012,** *51*, 6005-6008.
15. Kiejna, A.; Nieminen, R. M., Density-functional study of oxygen adsorption on Mo (112). *The Journal of chemical physics* **2005,** *122* (4), 044712.
16. Sierka, M.; Todorova, T. K.; Sauer, J.; Kaya, S.; Stacchiola, D.; Weissenrieder, J.; Shaikhutdinov, S.; Freund, H.-J., Oxygen adsorption on Mo (112) surface studied by ab initio genetic algorithm and experiment. *The Journal of chemical physics* **2007,** *126* (23), 234710.
17. Gautier, S.; Steinmann, S. N.; Michel, C.; Fleurat-Lessard, P.; Sautet, P., Molecular adsorption at Pt (111). How accurate are DFT functionals? *Physical Chemistry Chemical Physics* **2015,** *17* (43), 28921-28930.
18. Nørskov, J. K.; Abild-Pedersen, F.; Studt, F.; Bligaard, T., Density functional theory in surface chemistry and catalysis. *Proceedings of the National Academy of Sciences* **2011,** *108* (3), 937-943.
19. Kundu, M.; Murata, Y., Growth of single-crystal SiO2 film on Ni (111) surface. *Applied physics letters* **2002,** *80* (11), 1921-1923.
20. Boscoboinik, J. A.; Yu, X.; Yang, B.; Fischer, F. D.; Włodarczyk, R.; Sierka, M.; Shaikhutdinov, S.; Sauer, J.; Freund, H. J., Modeling Zeolites with Metal-Supported Two-Dimensional Aluminosilicate Films. *Angewandte Chemie International Edition* **2012,** *51* (24), 6005-6008.
21. Zhong, J. Q.; Wang, M.; Akter, N.; Kestell, J. D.; Niu, T.; Boscoboinik, A. M.; Kim, T.; Stacchiola, D. J.; Wu, Q.; Lu, D., Ionization-Facilitated Formation of 2D (Alumino) Silicate–Noble Gas Clathrate Compounds. *Advanced Functional Materials* **2019,** *29* (20), 1806583.
22. Wang, M.; Zhou, C.; Akter, N.; Tysoe, W. T.; Boscoboinik, J. A.; Lu, D., Mechanism of the Accelerated Water Formation Reaction under Interfacial Confinement. *ACS Catalysis* **2020,** *10* (11), 6119-6128.
23. Prieto, M. J.; Klemm, H. W.; Xiong, F.; Gottlob, D. M.; Menzel, D.; Schmidt, T.; Freund, H. J., Water Formation under Silica Thin Films: Real-Time Observation of a Chemical Reaction in a Physically Confined Space. *Angewandte Chemie International Edition* **2018**.
24. Eads, C. N.; Boscoboinik, J. A.; Head, A. R.; Hunt, A.; Waluyo, I.; Stacchiola, D. J.; Tenney, S. A., Enhanced Catalysis under 2D Silica: A CO Oxidation Study. *Angewandte Chemie International Edition* **2021,** *60* (19), 10888-10894.
25. Zhong, J.-Q.; Kestell, J.; Waluyo, I.; Wilkins, S.; Mazzoli, C.; Barbour, A.; Kaznatcheev, K.; Shete, M.; Tsapatsis, M.; Boscoboinik, J. A., Oxidation and reduction under cover: chemistry at the confined space between ultrathin nanoporous silicates and Ru (0001). *The Journal of Physical Chemistry C* **2016,** *120* (15), 8240-8245.
26. Emmez, E.; Yang, B.; Shaikhutdinov, S.; Freund, H.-J., Permeation of a single-layer SiO2 membrane and chemistry in confined space. *The Journal of Physical Chemistry C* **2014,** *118* (50), 29034-29042.
27. Lichtenstein, L.; Heyde, M.; Ulrich, S.; Nilius, N.; Freund, H.-J., Probing the properties of metal–oxide interfaces: silica films on Mo and Ru supports. *Journal of Physics: Condensed Matter* **2012,** *24* (35), 354010.
28. Mak, K. F.; Lee, C.; Hone, J.; Shan, J.; Heinz, T. F., Atomically thin MoS 2: a new direct-gap semiconductor. *Physical Review Letters* **2010,** *105* (13), 136805.
29. Tongay, S.; Zhou, J.; Ataca, C.; Lo, K.; Matthews, T. S.; Li, J.; Grossman, J. C.; Wu, J., Thermally driven crossover from indirect toward

 © xxxx IOP Publishing Ltd

direct bandgap in 2D semiconductors: MoSe2 versus MoS2. *Nano letters* **2012,** *12* (11), 5576-5580.
30. Novoselov, K. S.; Jiang, D.; Schedin, F.; Booth, T.; Khotkevich, V.; Morozov, S.; Geim, A. K., Two-dimensional atomic crystals. *Proceedings of the National Academy of Sciences* **2005,** *102* (30), 10451-10453.
31. Büchner, C.; Wang, Z.-J.; Burson, K. M.; Willinger, M.-G.; Heyde, M.; Schlögl, R.; Freund, H.-J., A Large-Area Transferable Wide Band Gap 2D Silicon Dioxide Layer. *ACS nano* **2016,** *10* (8), 7982-7989.
32. Akter, N.; Wang, M.; Zhong, J.-Q.; Liu, Z.; Kim, T.; Lu, D.; Boscoboinik, J. A.; Stacchiola, D. J., Stabilization of Oxidized Copper Nanoclusters in Confined Spaces. *Topics in Catalysis* **2018,** *61* (5-6), 419-427.
33. Büchner, C.; Lichtenstein, L.; Stuckenholz, S.; Heyde, M.; Ringleb, F.; Sterrer, M.; Kaden, W. E.; Giordano, L.; Pacchioni, G.; Freund, H.-J., Adsorption of Au and Pd on ruthenium-supported bilayer silica. *The Journal of Physical Chemistry C* **2014,** *118* (36), 20959-20969.
34. Włodarczyk, R.; Sierka, M.; Sauer, J.; Löffler, D.; Uhlrich, J.; Yu, X.; Yang, B.; Groot, I.; Shaikhutdinov, S.; Freund, H.-J., Tuning the electronic structure of ultrathin crystalline silica films on Ru (0001). *Physical Review B* **2012,** *85* (8), 085403.
35. Schlexer, P.; Pacchioni, G.; Włodarczyk, R.; Sauer, J., CO adsorption on a silica bilayer supported on Ru (0001). *Surface Science* **2016,** *648*, 2-9.
36. Lindroos, M.; Pfnür, H.; Held, G.; Menzel, D., Adsorbate induced reconstruction by strong chemisorption: Ru (001) p (2× 2)-O. *Surface Science* **1989,** *222* (2-3), 451-463.
37. Pfnür, H.; Held, G.; Lindroos, M.; Menzel, D., Oxygen induced reconstruction of a close-packed surface: A LEED IV study on Ru (001)-p (2× 1) O. *Surface Science* **1989,** *220* (1), 43-58.
38. Stampfl, C.; Schwegmann, S.; Over, H.; Scheffler, M.; Ertl, G., Structure and stability of a high-coverage (1× 1) oxygen phase on Ru (0001). *Physical Review Letters* **1996,** *77* (16), 3371.
39. Bleakley, K.; Hu, P., A density functional theory study of the interaction between CO and O on a Pt Surface: CO/Pt (111), O/Pt (111), and CO/O/Pt (111). *Journal of the American Chemical Society* **1999,** *121* (33), 7644-7652.
40. Eichler, A.; Hafner, J., Molecular precursors in the dissociative adsorption of O 2 on Pt (111). *Physical review letters* **1997,** *79* (22), 4481.
41. Materer, N.; Starke, U.; Barbieri, A.; Döll, R.; Heinz, K.; Van Hove, M.; Somorjai, G. A., Reliability of detailed LEED structural analyses: Pt (111) and Pt (111)-p (2× 2)-O. *Surface Science* **1995,** *325* (3), 207-222.
42. Conrad, H.; Ertl, G.; Küppers, J.; Latta, E., Interaction of NO and O2 with Pd (111) surfaces. II. *Surface Science* **1977,** *65* (1), 245-260.
43. Légaré, P.; Hilaire, L.; Maire, G.; Krill, G.; Amamou, A., Interaction of oxygen and hydrogen with palladium. *Surface Science* **1981,** *107* (2-3), 533-546.
44. Voogt, E.; Mens, A.; Gijzeman, O.; Geus, J., Adsorption of oxygen and surface oxide formation on Pd (111) and Pd foil studied with ellipsometry, LEED, AES and XPS. *Surface science* **1997,** *373* (2-3), 210-220.
45. Todorova, M.; Reuter, K.; Scheffler, M., Oxygen overlayers on Pd (111) studied by density functional theory. *The Journal of Physical Chemistry B* **2004,** *108* (38), 14477-14483.
46. Wang, M.; Zhong, J.-Q.; Stacchiola, D. J.; Boscoboinik, J. A.; Lu, D., First-principles study of interface structures and charge rearrangement at the aluminosilicate/Ru (0001) heterojunction. *The Journal of Physical Chemistry C* **2018,** *123* (13), 7731-7739.
47. Kresse, G.; Furthmüller, J., Efficient iterative schemes for ab initio total-energy calculations using a plane-wave basis set. *Physical Review B* **1996,** *54* (16), 11169.
48. Kresse, G.; Furthmüller, J., Efficiency of ab-initio total energy calculations for metals and semiconductors using a plane-wave basis set. *Computational Materials Science* **1996,** *6* (1), 15-50.
49. Bjorkman, T., Testing several recent van der Waals density functionals for layered structures. *J Chem Phys* **2014,** *141* (7), 074708.
50. Berland, K.; Hyldgaard, P., Exchange functional that tests the robustness of the plasmon description of the van der Waals density functional. *Physical Review B* **2014,** *89* (3), 035412.
51. Neugebauer, J.; Scheffler, M., Adsorbate-substrate and adsorbate-adsorbate interactions of Na and K adlayers on Al (111). *Physical Review B* **1992,** *46* (24), 16067.
52. Hamada, I.; Otani, M., Comparative van der Waals density-functional study of graphene on metal surfaces. *Physical Review B* **2010,** *82* (15), 153412.
53. Lee, K.; Murray, É. D.; Kong, L.; Lundqvist, B. I.; Langreth, D. C., Higher-accuracy van der Waals density functional. *Physical Review B* **2010,** *82* (8), 081101.

 © xxxx IOP Publishing Ltd

54. Boscoboinik, J. A.; Yu, X.; Yang, B.; Shaikhutdinov, S.; Freund, H.-J., Building blocks of zeolites on an aluminosilicate ultra-thin film. *Microporous and mesoporous materials* **2013,** *165*, 158-162.

 © xxxx IOP Publishing Ltd

Supplementary Materials

Exfoliating silica bilayers via intercalation at the silica/transition metal interface

Mengen Wang[1,2], J. Anibal Boscoboinik[1], and Deyu Lu[1*]

[1] Center for Functional Nanomaterials, Brookhaven National Laboratory, Upton, NY 11973, United States.
[2] Materials Science and Chemical Engineering Department, Stony Brook University, Stony Brook, NY 11790, United States.

E-mail: dlu@bnl.gov

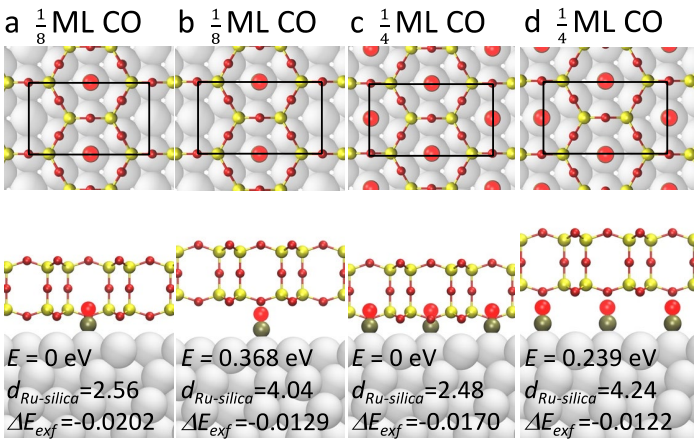

Figure S1. Top (*top*) and side (*bottom*) view of the relaxed structures of silica/*n*/Ru(0001) with the CO coverage of $\frac{1}{8}$ ML CO (a and b) and $\frac{1}{4}$ ML CO (c and d). *Color code*: Ru (white), Si (yellow), O (red) and C (tan). *E* is the total energy difference between the system where CO molecules cannot (a and c) or can (b and d) lift up the silica bilayer. $d_{Ru\text{-}silica}$ (Å) represents the interface distance and ΔE_{exf} (eV/Å^2) is the exfoliation energy.

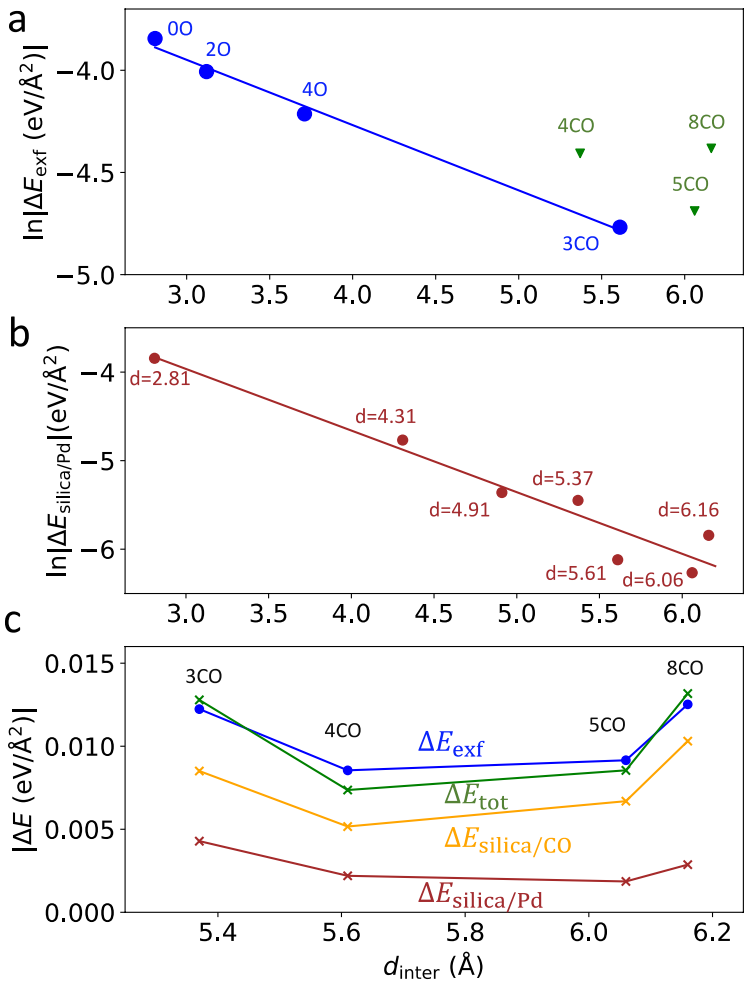

Figure S2. (a) The absolute value of the exfoliation energies ($|\Delta E_{exf}|$ in blue) and interaction energies ($|\Delta E_{Pd\text{-}silica}|$ in brown) between Pd(111) and BL-silica versus the interface distances ($d_{Pd\text{-}silica}$). (b) The absolute value of the exfoliation energies ($|\Delta E_{exf}|$ in blue), interaction energies between Pd(111) and BL-silica ($|\Delta E_{Pd\text{-}silica}|$ in brown), interaction energies between CO and BL-silica ($|\Delta E_{CO\text{-}silica}|$ in red) and the sum of $|\Delta E_{Pd\text{-}silica}|$ and $|\Delta E_{CO\text{-}silica}|$ (green) versus $d_{Pd\text{-}silica}$ for BL-silica/CO/Pd (111). All the energies are in eV/Å^2.

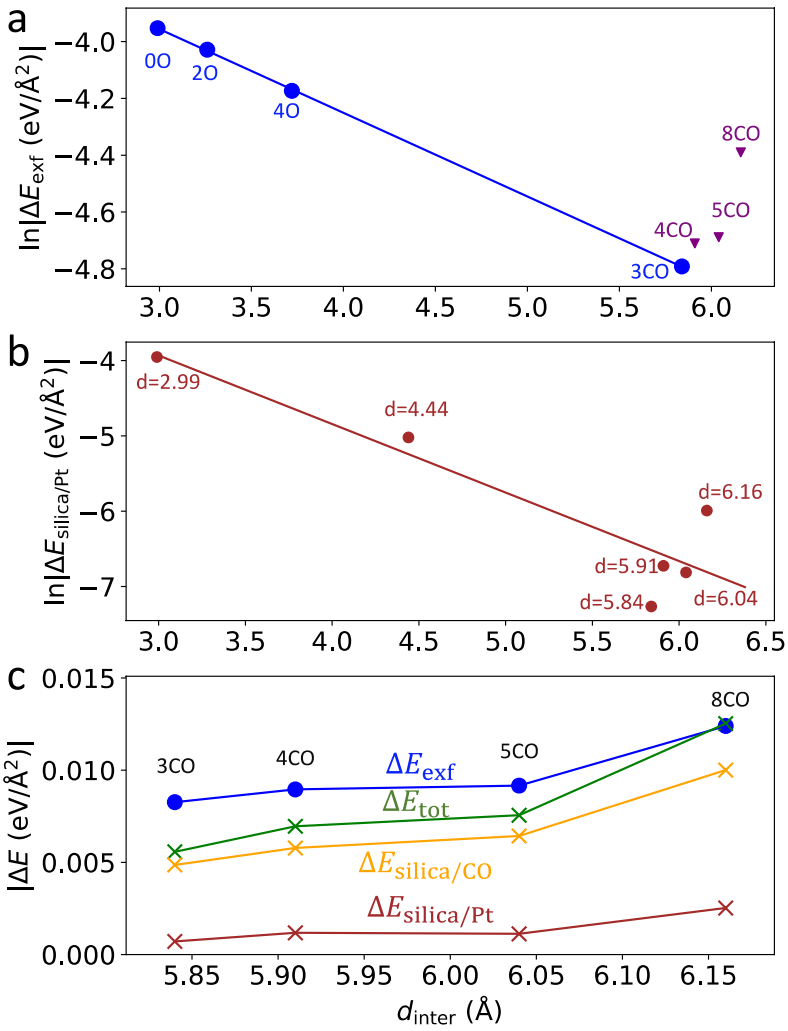

Figure S3. (a) The absolute value of the exfoliation energies ($|\Delta E_{exf}|$ in blue) and interaction energies ($|\Delta E_{Pt\text{-}silica}|$ in brown) between Pt(111) and BL-silica versus the interface distances ($d_{Pt\text{-}silica}$). (b) The absolute value of the exfoliation energies ($|\Delta E_{exf}|$ in blue), interaction energies between Pt(111) and BL-silica ($|\Delta E_{Pt\text{-}silica}|$ in brown), interaction energies between CO and BL-silica ($|\Delta E_{CO\text{-}silica}|$ in red) and the sum of $|\Delta E_{Pt\text{-}silica}|$ and $|\Delta E_{CO\text{-}silica}|$ (green) versus $d_{Pt\text{-}silica}$ for BL-silica/CO/Pt(111). Similar to BL-silica/Ru(0001), there is no decrease in $|\Delta E_{exf}|$ even if $d_{Pd\text{-}silica}$ or $d_{Pt\text{-}silica}$ further increases at $n_{CO} \geq 3$. All the energies are in eV/Å^2.

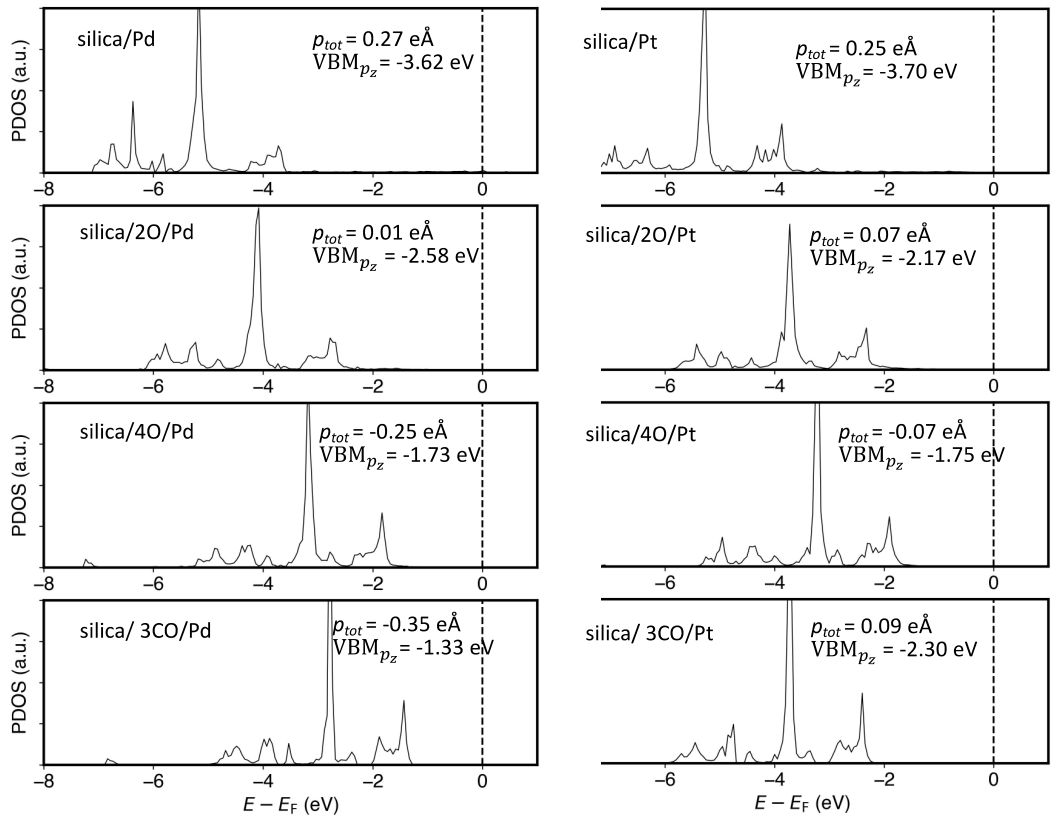

Figure S4. Projected density of states of p_z orbitals of the bottom layer O atoms. p_{tot} represent the total dipole moment of the system. VBM_{p_z} is the valence band maximum of the p_z orbital. ϵ_p is the O_{bot} p_z band center and $\Delta\epsilon_p = \epsilon_p - VBM_{p_z}$ is the p_z band center shift. The energies are relative to the Fermi level.